

## RESEARCH ARTICLE

# Substrate availability and not thermal acclimation controls microbial temperature sensitivity response to long-term warming

Luiz A. Domeignoz-Horta<sup>1,2</sup>  | Grace Pold<sup>3</sup>  | Hailey Erb<sup>1</sup>  | David Sebag<sup>4,5</sup>  |  
 Eric Verrecchia<sup>5</sup> | Trent Northen<sup>6,7</sup> | Katherine Louie<sup>7</sup>  | Emiley Eloe-Fadrosh<sup>7</sup>  |  
 Christa Pennacchio<sup>7</sup> | Melissa A. Knorr<sup>8</sup> | Serita D. Frey<sup>8</sup>  | Jerry M. Melillo<sup>9</sup> |  
 Kristen M. DeAngelis<sup>1</sup> 

<sup>1</sup>Department of Microbiology, University of Massachusetts, Amherst, Massachusetts, USA

<sup>2</sup>Department of Evolutionary Biology and Environmental Studies, University of Zurich, Zurich, Switzerland

<sup>3</sup>Department of Forest Mycology and Plant Pathology, Swedish University of Agricultural Sciences, Uppsala, Sweden

<sup>4</sup>IFP Energies Nouvelles, Rueil-Malmaison, France

<sup>5</sup>Faculty of Geosciences and the Environment, Institute of Earth Surface Dynamics, University of Lausanne, Lausanne, Switzerland

<sup>6</sup>Environmental Genomics and Systems Biology Division, Lawrence Berkeley National Laboratory, Berkeley, California, USA

<sup>7</sup>The DOE Joint Genome Institute, Lawrence Berkeley National Laboratory, Berkeley, California, USA

<sup>8</sup>School of Natural Resources and the Environment, University of New Hampshire, Durham, New Hampshire, USA

<sup>9</sup>The Ecosystems Center, Marine Biological Laboratories, Woods Hole, Massachusetts, USA

## Correspondence

Luiz A. Domeignoz-Horta, Department of Evolutionary Biology and Environmental Studies, University of Zürich, Winterthurerstrasse 190, 8057 Zürich, Switzerland.  
 Email: [luiz.domeignoz-horta@ieu.uzh.ch](mailto:luiz.domeignoz-horta@ieu.uzh.ch)

## Funding information

Joint Genome Institute, Grant/Award Number: 506489; National Science Foundation, Grant/Award Number: DEB-1456528, DEB-1749206 and DEB-1832210

## Abstract

Microbes are responsible for cycling carbon (C) through soils, and predicted changes in soil C stocks under climate change are highly sensitive to shifts in the mechanisms assumed to control the microbial physiological response to warming. Two mechanisms have been suggested to explain the long-term warming impact on microbial physiology: microbial thermal acclimation and changes in the quantity and quality of substrates available for microbial metabolism. Yet studies disentangling these two mechanisms are lacking. To resolve the drivers of changes in microbial physiology in response to long-term warming, we sampled soils from 13- and 28-year-old soil warming experiments in different seasons. We performed short-term laboratory incubations across a range of temperatures to measure the relationships between temperature sensitivity of physiology (growth, respiration, carbon use efficiency, and extracellular enzyme activity) and the chemical composition of soil organic matter. We observed apparent thermal acclimation of microbial respiration, but only in summer, when warming had exacerbated the seasonally-induced, already small dissolved organic matter pools. Irrespective of warming, greater quantity and quality of soil

Luiz A. Domeignoz-Horta and Grace Pold contributed equally to this work.

This is an open access article under the terms of the [Creative Commons Attribution-NonCommercial-NoDerivs](https://creativecommons.org/licenses/by-nc-nd/4.0/) License, which permits use and distribution in any medium, provided the original work is properly cited, the use is non-commercial and no modifications or adaptations are made.

© 2022 The Authors. *Global Change Biology* published by John Wiley & Sons Ltd.

carbon increased the extracellular enzymatic pool and its temperature sensitivity. We propose that fresh litter input into the system seasonally cancels apparent thermal acclimation of C-cycling processes to decadal warming. Our findings reveal that long-term warming has indirectly affected microbial physiology via reduced C availability in this system, implying that earth system models including these negative feedbacks may be best suited to describe long-term warming effects on these soils.

#### KEYWORDS

carbon use efficiency, climate change, microbial temperature sensitivity, microbial thermal acclimation, soil carbon cycling

## 1 | INTRODUCTION

Microbes are key regulators of Earth's massive soil carbon stocks, determining the partitioning of plant inputs into soil organic matter (SOM) versus atmospheric carbon dioxide. Climate warming is liable to accelerate microbial activity, changing not only the magnitude but also the composition of SOM stocks. However, the degree to which warming will accelerate microbial activity and alter SOM quantity and quality remains uncertain, in part because of insufficient understanding of how the soil–microbe system may acclimate to warming (Bradford et al., 2008; Cavicchioli et al., 2019; Melillo et al., 2017; Walker et al., 2018, 2020).

Thermal acclimation is the divergence between long- and short-term responses to temperature occurring at the community level, which plays out as a change in the slope of the relationship between temperature and microbial process rate, or “temperature sensitivity.” Thermal acclimation can be driven by and seen at scales occurring from subcellular to ecosystem scales (Bradford et al., 2008). Observed community thermal acclimation can be the result of both direct and indirect responses to temperature. Direct responses include changes in protein or membrane stability at the cellular level (Bradford, 2013; Hall et al., 2010), and shifts in the extracellular enzyme pool toward isoenzymes characterized by distinct activation energies and temperature optima (Davidson & Janssens, 2006; Robinson et al., 2017). Indirect drivers of community thermal acclimation can also include changes in resource composition and supply (Kirschbaum, 2004; Moinet et al., 2021; Pold et al., 2016), whose effects on microbial physiology can act through changes in soil microbial community structure (Rocca et al., 2019) and/or reduction of bacterial cellular ribosome content (Sollinger et al., 2022). By shaping the degree to which microbial processes responsible for soil C cycling vary with temperature, thermal acclimation can determine whether soils serve as a source or sink for carbon (Allison et al., 2010).

Nonetheless, community thermal acclimation is not a necessary outcome of exposure to long-term elevated temperatures (Allison et al., 2018; Carey et al., 2016), in part because substrate quantity and quality may change concurrently (Alster et al., 2022). Perhaps the most responsive and dynamic of these pools, dissolved organic

matter (DOM), consists of compounds derived both directly from root and mycorrhizal exudates and leaf litter leachate, and indirectly from decomposition of SOM and the turnover of microbial biomass (Bolan et al., 2011; Malik & Gleixner, 2013). The magnitude and relevance of these DOM sources are also expected to change seasonally as plant and microbial inputs changes through seasons (Cheeke et al., 2021; Wardle et al., 2004; Yarwood et al., 2009), meaning that any effect of warming is overlain on existing variation in substrate scarcity and abundance for microbes. Furthermore, since metabolic rates increase with temperature until reaching their optima (Alster et al., 2022; Ratkowsky et al., 1982), microbial substrate demand is also expected to increase at elevated temperatures (Price & Sowers, 2004). However, not all substrates are equally able to meet microbial demand, whether it be due to differences in enzyme investment required to access them, activation energy needed to be overcome to decompose them, adenosine triphosphate (ATP) required to uptake them, or cellular reducing equivalents required to assimilate them (Gommers et al., 1988; Gunina & Kuzyakov, 2022). Notably, the most energetically rich compounds are not necessarily the most favorable to consume due to the resources which must be invested into extracellular enzymes to access them (Gunina & Kuzyakov, 2022; LaRowe & Van Cappellen, 2011), thereby reducing carbon use efficiency (CUE)—or the proportion of carbon taken up that is ultimately assimilated into biomass. Furthermore, SOM components can differ in how sensitive their decomposition is to temperature, leading to considerable changes in SOM chemistry under chronic warming (Feng et al., 2008; Pec et al., 2021; Pold et al., 2017; VandenEnden et al., 2021). These long-term warming-induced changes in SOM chemistry are in turn expected to alter the potential resource pool (i.e., DOM) available for organisms to respond to short-term changes in temperature (Liu et al., 2021). Since microbial community members differ in their ability to consume various components of DOM (Zhalnina et al., 2018), substrate-dependent responses of microbial physiology to temporary increases in temperature can emerge (Frey et al., 2013). While numerous studies have linked substrate depletion to changes in the apparent temperature sensitivity of microbial respiration (Alster et al., 2022; Bradford et al., 2008; Hartley et al., 2007; Moinet et al., 2021), there is an acute need to understand how potential changes in substrate chemistry under climate warming can affect soil microbial activity.

Here we evaluated the hypothesis that long-term warming indirectly affects microbial physiology via reductions in the quantity and quality of carbon. This is based on the premise that warming can reduce SOM quality (Feng et al., 2008; Pec et al., 2021; Pold et al., 2017; VandenEnden et al., 2021) and that SOM quality constrains microbial physiology (Gommers et al., 1988). To test this hypothesis, we took soils from two long-term soil warming experiments in a temperate deciduous forest, sampled during summer and autumn, and completed laboratory-based assays of SOM characterization and microbial physiology under a range of temperatures.

## 2 | METHODS

### 2.1 | Soil collection

Soils were collected from two long-term warming experiments at the Harvard Forest Long-Term Ecological Research (LTER) sites in Petersham MA USA (42°30'30"N, 72°12'28"W). The two experiments are located immediately adjacent to each other and had been warmed +5°C for 13 (Soil Warming and Nitrogen Addition Study [SWaN]; Contosta et al., 2011) or 28 years (Prospect Hill [PH]; Melillo et al., 2002). We sampled control and heated plots in SWaN, and disturbance control and heated plots in PH; these disturbance controls had heating cables buried as in the heated plots, but the power was never turned on. Experimental plots are 6×6 m at Prospect Hill, and 3×3 m at SWaN, and follow a randomized block design in the former and a completely randomized design in the latter.

The sites of the two warming experiments are co-located in the same forest stand, characterized by coarse-loamy inceptisols and the same dominant tree species: paper and black birch (*Betula papyrifera* and *lenta*), red maple (*Acer rubrum*), black and red oak (*Quercus velutina* and *rubra*), and American beech (*Fagus grandifolia*). SWaN plots are situated under a canopy gap relative to PH, resulting in slightly different understory vegetation between the two sites (Muth & Bazzaz, 2002). We pooled the control plot data from both sites for analysis since the control plots do not differ in the parameters measured here, with the exception of SOM lability index (l index). However, warmed treatment plots at SWaN and PH have not followed the same respiration trajectory over the course of the experiment, so we do not consider the field experiments as two stages in a chronosequence. Additional site details can be found in Table S1.

Soils were sampled on 15 July and 19 October 2019, timings which were chosen to reflect soil processes before and after autumn litter deposition (Munger & Wofsy, 2021). We observed that between July and October of 2019, most of the *Acer* trees had lost their leaves, resulting in an increase in forest floor litter material between the two time points.

Two 10 cm depth soil cores were collected from each of five plots per site, treatment, and time point using a 5.7 cm diameter tulip bulb planter. After removing and excluding the undecomposed forest floor litter material, these cores were separated into organic and mineral

soil by color and texture. Soils were then sieved to 2 mm on site and transported back to the laboratory at ambient temperature, within 4 h of collection (Figure 1a). We ultimately processed and analyzed a total of 79 samples because the organic soil exceeded the length of the corer and prevented sampling of the mineral soil in one control SWaN plot in July. Immediately upon arrival at the laboratory, different subsamples of soil were dried to constant mass at 65°C overnight to determine soil moisture content or placed in the -80°C for metabolomic analysis. The remaining soil was left in plastic containers at room temperature (20°C) overnight. Samples which had greater than the target of 48% water holding capacity were left with the lids of the container ajar to allow them to dry slightly overnight ( $n = 2$  samples). Soil was then weighed for the CUE, respiration, enzyme assays, microbiological assays, and SOM analyses described below (Figure 1).

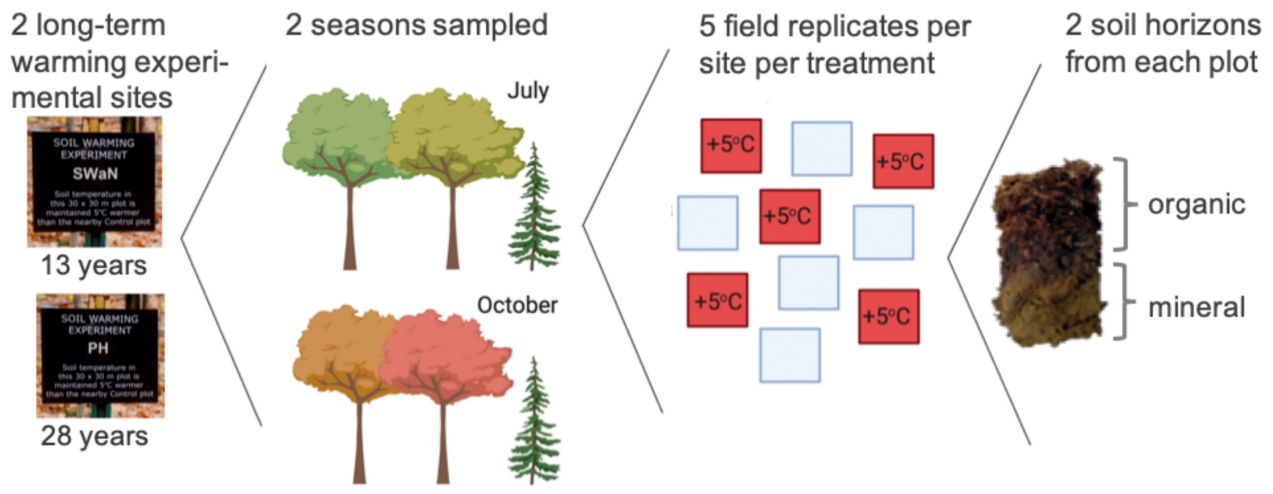
### 2.2 | Microbial community catabolic potential

We used BioLog Ecoplates to evaluate the intrinsic potential growth rate and substrate preferences of microbes in our soil samples. Within 24 h of collecting soils, we placed 0.25 g (organic) or 0.5 g (mineral) soil in a 125 ml Erlenmeyer flask with 50 ml of 0.9% sodium chloride and mixed on a shaker table at 180 rpm for 30 min. The flasks were then left for 5 min to allow the particles to settle, and then 100 µl of supernatant was transferred to each well of the EcoPlate. The initial absorbance of each plate was measured at 590 and 750 nm and after every 4–12 h afterwards to capture the full growth curves. The measurements at 750 nm were subtracted from the measurements at 590 nm to differentiate the change in dye reduction through time from the change in cell growth. Then the amount of dye color development in the water only well was subtracted out to quantify the metabolic activity due to the substrate itself. Negative control plates containing just buffer were used to verify the assays were not contaminated. We subsequently fit growth curves to both individual substrates and to the average color across the plate (mean well color development) using the *growthcurver* package (Sprouffske & Wagner, 2016). Growth rates not significantly different from zero ( $p > .05$ ) were set to zero before all substrate-specific growth rates were used for calculating substrate class-specific growth rates and for principal coordinates analysis. Principal coordinates analysis was completed using the *vegan* package (Oksanen et al., 2019) with a Hellinger-transformed relative growth rate matrix rather than the raw growth rate data so that relative substrate preference could be separated from the overall differences in growth rate under the assay conditions. We refer to the first axis of this ordination as the “ecoplate substrate diversity.”

### 2.3 | Extracellular enzyme activity

Between the collection and completion of extracellular enzyme assays (within 4 days), we stored soils at 15°C, which was near the middle

## (a) Sampling design:



## (b) Experimental design:

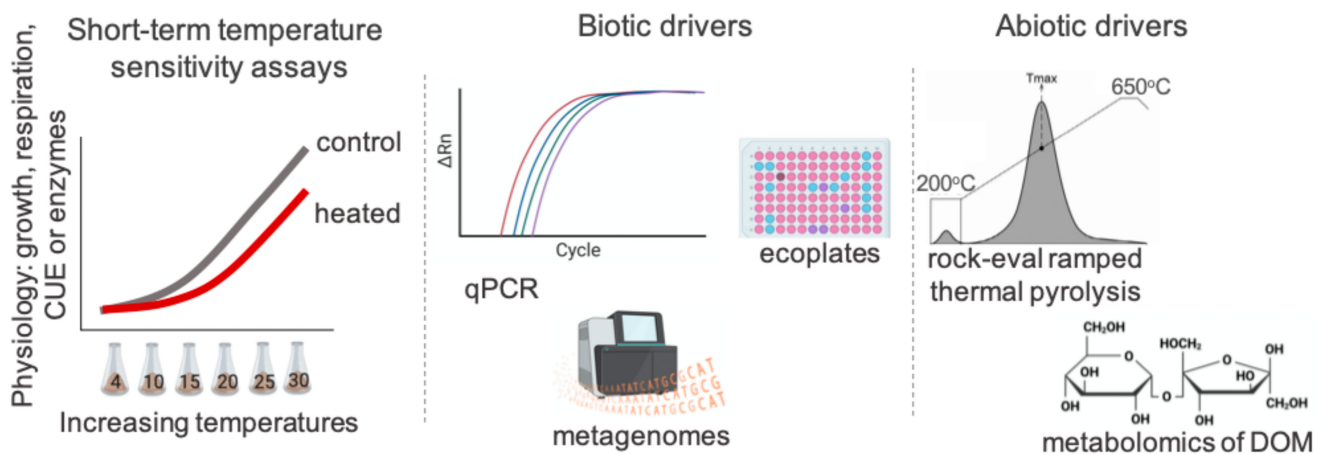


**FIGURE 1** Experimental design. Sampling design (a). Samples were harvested at two time points in July and October 2019 at two long-term warming experiments SWaN and PH at the Harvard Forest long-term ecological research station (LTER) which had been established for 13 and 28 years, respectively. From each experimental site, soil cores were harvested from five replicated warm plots, heated 5°C above ambient soil and control soils. Each soil core was subdivided into organic and mineral horizons. Laboratory assays (b). First, temperature sensitivity assays were performed with respiration, growth ( $^{18}\text{O}$ -water method), carbon use efficiency (CUE), and extracellular enzyme activities (beta-glucosidase, *N*-acetylglucosaminidase, oxidative enzyme activities). Second, we also determined the abundance of fungal and bacterial cells with real-time PCR (RT-PCR); evaluated the potential growth on Biolog EcoPlates at the soil temperature in the moment of sampling (e.g., 20 and 25°C for July and 15 and 20°C for October for both heated and control soils); measured the metabolomics and the metagenomes in a subset of data. Finally, we measured the soil organic matter quality with the rock-eval® thermal pyrolysis and quantified the dissolved organic carbon in soil extracts.

of field temperature range. We assayed the cellulose-degrading enzyme beta-glucosidase (BG), the chitin- and peptidoglycan-degrading enzyme *N*-acetylglucosaminidase (NAG), and the oxidative enzyme pool (phenol oxidase + peroxidase; OX) at 4, 10, 15, 20, 25, and 30°C, covering most of the range of growing season temperatures experienced by heated and control plot soil communities at these sites. These enzymes were selected for their propensity to target chemically similar (BG) or chemically diverse (OX) bonds, as well as microbial necromass (NAG) (Burns & Dick, 2002).

Slurries were prepared with 1.25 g fresh wet weight soil in 175 ml 50 mM pH 4.7 sodium acetate buffer, using a Waring blender set to

high for 1 min. The slurry was stirred at 300 rpm during pipetting to ensure an even distribution of soil. Fourteen technical replicates of 200  $\mu\text{l}$  slurry were pipetted into black plates for BG and NAG, and 500  $\mu\text{l}$  into deep well 2 ml plates for total oxidative enzyme pool. Plates were placed at the assay temperature for at least 25 min before substrate addition to allow them to reach the specific target temperature. Fifty microliter of 4000  $\mu\text{M}$  4-methylumbelliferyl  $\beta$ -D-glucopyranoside or 2000  $\mu\text{M}$  4-methylumbelliferyl *N*-acetyl- $\beta$ -D-glucosaminide, or 500  $\mu\text{l}$  25 mM L-DOPA + 0.03%  $\text{H}_2\text{O}_2$  were added to each well, which we previously deemed to be sufficient to attain the maximum activity rate. Each hydrolytic plate contained a

slurry-only control (200  $\mu$ l slurry, 50  $\mu$ l buffer) and a standard curve (50  $\mu$ l 0–500  $\mu$ M in twofold dilution, in 200  $\mu$ l buffer). A separate plate for mineral and organic soil quenches (200  $\mu$ l slurry, 50  $\mu$ l standard) and substrate-only controls (200  $\mu$ l buffer, 50  $\mu$ l substrate) was prepared for each temperature.

Hydrolytic assay plates were measured at an excitation/emission wavelength pair of 360/450 nm immediately following substrate addition and after an additional 2, 4, and 8 h. Greatest activity was observed between 0 and 2 h, so we used data from this period in our analyses. A 100  $\mu$ l aliquot of the supernatant from oxidative assay plates was removed to a clear polystyrene plate after 4 h of incubation and read at 460 nm. We used a SpectraMax M2 plate reader controlled by the SoftMaxPro v. 5.4 software for all measurements. Extracellular enzyme rates were calculated as previously (German et al., 2011) and normalized by the sample-specific microbial biomass carbon (MBC) measurement (described below).

## 2.4 | Respiration, growth, and CUE

We used the substrate-independent ( $\text{H}_2^{18}\text{O}$ -CUE) method (Spohn et al., 2016) to evaluate soil microbial CUE. Weighing for growth and respiration measurements began the day following soil collection. Three 0.3 g (mineral) or 0.15 g (organic) replicate aliquots of soil were weighed into small vials, placed in a larger tube, and sealed with parafilm to prevent additional moisture loss. Once all samples were weighed (2 days after soil collection), water was added to bring them to 60% water holding capacity. Two replicates received water so that 20% of the total water was present as  $^{18}\text{O}$ -water, while the remaining replicate received all water as  $^{16}\text{O}$ -water to account for natural abundance  $^{18}\text{O}$ . Tubes were stoppered with a neoprene bung and immediately placed in the appropriate incubator (4, 10, 15, 20, 25, or 30°C). Empty tubes were also sealed after every 5–10 tubes in order to measure the starting  $\text{CO}_2$  levels in tubes. After 24 (15–30°C) or 48 (4 and 10°C) hours, the  $\text{CO}_2$  was measured in the tube using a 30 ml headspace sample injected into a Quantek instruments infrared gas analyzer with 10 ppm sensitivity. We used a longer time for the lower temperatures because preliminary incubations indicated that it was necessary to reliably detect respiration. The soil samples were placed at –80°C until DNA extraction. We also incubated larger quantities of soil in order to validate respiration measurements from the CUE incubations. One gram (organic) or 2 g (mineral) soil were brought to 60% water holding capacity with  $^{16}\text{O}$ -water, and the tubes were incubated alongside the CUE samples.

CUE measurements using the ( $\text{H}_2^{18}\text{O}$ -CUE) method estimate the new microbial biomass produced during the incubation period based on  $^{18}\text{O}$ -DNA at the end of the incubation period. DNA was extracted from all soils incubated with  $^{18}\text{O}$ -water and a subset of soils incubated with  $^{16}\text{O}$ -water using the Qiagen Powersoil kit. Technical duplicates were pooled before quantification using Qubit. The  $^{18}\text{O}$  enrichment of the DNA was measured using TC/EA-IRMS (Delta V Advantage, Thermo Fisher) at the UC Davis Stable Isotope Facility. CUE was calculated as per Spohn et al. (2016) but using a sample-specific

conversion factor rather than the overall average because large differences in MBC:DNA ratios across community types can bias CUE measurements (Pold, Domeignoz-Horta & DeAngelis, 2020).

## 2.5 | Temperature response curve fitting

We anticipated that respiration and extracellular enzyme activity would increase non-linearly with incubation temperature. Therefore, we compared fits of the Taylor exponential model (Lloyd & Taylor, 1994;  $\ln[\text{rate}] = \ln[a] + b \times \text{Temperature}$ ), and the Ratkowsky square root model (Ratkowsky et al., 1982;  $\sqrt{\text{rate}} = b[T - T_0]$ ) to these data. Models for respiration were fit to individual soil samples using the  $\text{lm}()$  function in R where the response variable (i.e., respiration or extracellular enzyme activity) was either natural log- or square root transformed. We extracted the slope (i.e., temperature sensitivity;  $b$  in equations above) estimates from the model for each sample to compare among experimental factors.

Visually, the Ratkowsky model consistently underestimated the respiration at higher temperatures compared to the Taylor model, and the  $R^2$  statistic was also consistently lower (median  $R^2 = .91$  [range 0.65–0.98] versus 0.96 [range 0.66–0.99], median difference = 0.052; Table S3). Therefore, we proceeded to extract the slope parameter from the Taylor model and used this as a metric of temperature responsiveness for downstream statistical analyses for both respiration and extracellular enzyme activity. For BG, the  $R^2$  for the Taylor model varied from 0.42 to 0.99, with a median of 0.85. For NAG,  $R^2$  varied from 0.04 to 0.99 with a median of 0.85 (Table S4). Since all  $R^2$  below .4 were restricted to October, we excluded NAG activity from this time for our analysis. The Taylor model similarly showed a poor fit to the oxidative enzyme activity (median  $R^2 = .88$ , range .00–.99) with instances of poor fit seen in data from both time points. Therefore, we did not further analyze oxidative enzyme activity temperature sensitivity (Table S4). The growth and CUE data were very variable compared to the respiration data and individual samples did not follow a consistent pattern. Therefore, we could not fit a curve to the data and instead used ranked CUE and growth rates at different temperatures for each soil sample. We considered the CUE temperature optimum to be the temperature where we measured its highest value (Bölscher et al., 2020).

## 2.6 | Quantitative PCR

The abundance of total fungi and total bacteria was assessed using quantitative PCR (qPCR) with ITS primers (ITS1: 5'-TCCGT AGGTGAACCTGCGG-3' and 5.8S: 5'-CGCTGCGTTCATCG-3') and 16S ribosomal RNA primers (Eub338: 5'-ACTCCTACGGGAG GCAGCAG-3' and Eub518: 5'-ATTACCGCGTCTGCTGG-3') (Fierer et al., 2005), respectively. The abundance in each soil sample was based on increasing fluorescence intensity of the SYBR Green dye during amplification. The qPCR assay was carried out in a 15  $\mu$ l reaction volume containing 2 ng of DNA, 7.5  $\mu$ l of SYBR Green PCR

master mix (Qiagen quantifast SYBR kit), and each primer at a concentration of 1  $\mu\text{M}$ . Inhibition tests were performed by running serial dilutions of DNA extractions and did not indicate inhibition of amplification. For each sample at least two independent qPCR assays were performed for each gene with technical duplicates within each assay. The qPCR efficiencies for both genes ranged between 78% and 110%. Values are reported as gene copy number  $\text{g}^{-1}$  dry soil.

## 2.7 | Microbial biomass carbon

Quadruplicate 0.5 g (organic) or 1 g (mineral) soil samples for MBC were weighed out with the CUE samples. We kept the weighed out soil samples at 15°C (the middle of the temperature range used for CUE and enzyme measurements) until the end of CUE incubations so growth and biomass measurements could be taken on similarly treated soils. Two replicates were exposed to chloroform vapor fumigation under vacuum for 24 h, while the other two replicates were placed at 4°C for the duration. Soils with and without chloroform were subsequently extracted in 15 ml of 0.05 M  $\text{K}_2\text{SO}_4$ , which a preliminary trial indicated led to similar levels of extractable organic carbon and MBC detected as the more standard 0.5 M  $\text{K}_2\text{SO}_4$  for our soils. DOC was measured on a Shimadzu TOC analyzer.

## 2.8 | SOM quality

We used ramped thermal rock-eval® pyrolysis (RE) to evaluate SOM quality (Soucémariadin et al., 2018). During RE, carbon oxides are quantified as they come off a soil sample subject to increasing temperatures, thereby providing a metric of SOM intrinsic thermal stability. Compounds with high thermal stability include aromatic and phenolic non-lignin compounds, while lipids and polysaccharides tend to have lower thermal stability (Sanderman & Grandy, 2020). Mineral and organic soils were dried at 65°C and crushed to a fine powder in a mortar and pestle. Between 50 and 70 mg soil was pyrolyzed over a temperature ramp from 200 to 650°C, followed by combustion to 850°C using a rock-eval 6 pyrolyzer (Vinci technologies) at the Institute of Earth Sciences of the University of Lausanne (Switzerland). Hydrocarbons released during this process were measured by a flame ionization detector. The resultant thermogram was used to calculate the I index ("labile carbon fraction") and R index ("recalcitrant carbon fraction") as previously (Sebag et al., 2016). We also used the thermogram of each sample to calculate a Bray–Curtis distance matrix of all samples, taking the peak height at each 1°C increment as an input value to create the distance matrix between all samples (Domeignoz-Horta et al., 2021). This approach allowed us to evaluate SOM composition in addition to C quantities in the different soils. The first axis of the NMDS was used as a proxy for SOM quality as it was strongly correlated with the I index ( $R^2 = .89$ ,  $p < .0001$ ).

## 2.9 | Metabolomics

Water-extractable polar metabolites (here, "water-extractable organic matter," or WEOM) were obtained by shaking 1 g dry soil equivalent with 5 ml (mineral soil) or 10 ml (organic soil) of LC/MS-grade water at 200 rpm and 4°C for 1 h. Every extraction was accompanied with a water-only control. The soil extracts and the water controls were filtered through a 45  $\mu\text{m}$  PTFE filter. The filtrate was lyophilized and sent for analysis at the DOE Joint Genome User Facility at Lawrence Berkeley National Laboratory. Polar metabolites were resuspended in 170  $\mu\text{l}$  of 100% methanol containing  $^{13}\text{C}$ - $^{15}\text{N}$  labeled amino acids (30 M, 767964, Sigma). UHPLC normal phase chromatography was performed using an Agilent 1290 LC stack, with MS and MS/MS data collected using a Q Exactive HF Orbitrap MS (Thermo Scientific). Full MS spectra were collected from  $m/z$  70–1050 at 60k resolution in both positive and negative ionization mode, with MS/MS fragmentation data acquired using stepped 10, 20, and 40 eV collision energies at 17,500 resolution. Mass spectrometer source settings included a sheath gas flow rate of 55 (au), auxiliary gas flow of 20 (au), sweep gas flow of 2 (au), spray voltage of 3 kV, and capillary temperature of 400°C. Normal phase chromatography was performed using a HILIC column (InfinityLab Poroshell 120 HILIC-Z, 2.1150 mm, 2.7 m, Agilent, 683775-924) at a flow rate of 0.45  $\text{ml min}^{-1}$  with a 2  $\mu\text{l}$  injection volume. To detect metabolites, samples were run on the column at 40°C equilibrated with 100% buffer B (99.8% 95:5 v/v ACN:H<sub>2</sub>O and 0.2% acetic acid, w/ 5 mM ammonium acetate) for 1 min, diluting buffer B down to 89% with buffer A (99.8% H<sub>2</sub>O and 0.2% acetic acid, w/ 5 mM ammonium acetate and 5 M methylene-di-phosphonic acid) over 10 min, down to 70% over 4.75 min, down to 20% over 0.5 min, and isocratic elution for 2.25 min, followed by column re-equilibration by returning to 100% B over 0.1 min and isocratic elution for 3.9 min. The injection order of the 79 experimental samples and 5 extraction controls was randomized and an injection blank (2  $\mu\text{l}$  of 100% MeOH) run between each sample. Metabolomics data were analyzed using Metabolite Atlas (Yao et al., 2015) and with in-house Python scripts to obtain extracted ion chromatograms and peak heights for each metabolite.

Metabolite identifications were verified with authentic chemical standards and validated based on three metrics comparing (1) detected versus theoretical  $m/z$  (<5 ppm), (2) retention time ( $\leq 0.5$  min), and (3) fragmentation spectra similarity to a chemical standard run using the same chromatography and LC-MS/MS method. Data from internal standards and quality control samples (included throughout the run) were analyzed to ensure consistent peak heights and retention times. Peak height of different samples was calculated out of four replicates and we excluded metabolites that showed a quality score under 1 and were not measured in every sample. Where multiple ions existed for the same compound within a sample analyses we summed the peak heights. Where compounds appeared in both the positive and the negatively charged compound summary table, we used the greatest value. After quality control we had 227 compounds. The WEOM matrix was normalized by sum and pareto scaled before

calculating Bray–Curtis distance and completing principal coordinates analysis using the *MetabolAnalyze*, *vegan* and *ape* packages, respectively (Nyamundanda et al., 2010; Oksanen et al., 2019; Paradis & Schliep, 2019). Pareto scaling divides each compound by the square root of the variance. We selected this scaling approach to moderately reduce the importance of the extremely dominant compounds and remove the large differences in total peak height between mineral and organic soil samples without completely abolishing all relative abundance information.

Compound complexity was determined based on the Bertz/Hendrickson/Ihlenfeldt complexity reported in PubChem. The complexity score is higher in polymers compared to monomers of the same compound, and in asymmetric and/or heteropolymeric compared to symmetric and/or homopolymeric compounds. Therefore, the complexity score can be considered an imprecise proxy for how difficult a compound is to break down. These values were downloaded from PubChem. Mean nominal oxidation state was calculated as per (LaRowe & Van Cappellen, 2011) ( $\text{NOSC} = -((-Z + 4C + H - 3N - 2O + 5P - 2S) / C) + 4$ ). NOSC was selected as a proxy for the quality of DOC because oxidation of compounds with higher NOSCs is associated with greater electron transfer (LaRowe & Van Cappellen, 2011), while compounds with lower NOSCs have greater potential energy but require a larger investment to acquire it. As such, the NOSC of SOM generally decreases as decomposition proceeds (Gunina & Kuzyakov, 2022). The NOSC and complexity indices for each compound are reported in Table S5.

## 2.10 | Metagenome sequencing and annotation

Metagenomes were obtained from organic soil collected in July from both sites, totaling 20 samples. DNA extracted from soils incubated at 20°C was sequenced at the Joint Genome Institute (Methods S1 and Table S2). Reads were assembled and PFAMs were annotated in the assembled fraction of reads using the DOE-JGI Metagenome Annotation Pipeline (Huntemann et al., 2016). This led to an average of 1.72 Gbp assembled and 2,807,085 genes predicted per metagenome. We then mapped PFAMs to CAZys (Pold et al., 2016) and used mean mapping depth for CAZys relative to the mapping depth to the single copy *rpoB* gene (PF04563, PF04561, PF04565, PF10385, PF00562, PF04560) as our proxy of CAZy abundance across samples. We elected to focus on CAZymes as they are responsible for the polymerization and depolymerization of many of the dominant compounds found in leaf litter and microbial cell walls, including cellulose, lignin, and chitin. We subsequently categorized CAZymes based on the primary substrates they decompose (Berlemont et al., 2015).

## 2.11 | Data analysis

Analysis was completed in R version 3.6.3 using packages *reshape2* (Wickham, 2007), *vegan* (Oksanen et al., 2019), *lme4*

(Pinheiro, et al., R Core Team, 2019), *agricolae* (Mendiburu, 2019), *grofit* (Kahm et al., 2010), *dplyr* (Wickham et al., 2022), *lattice* (Sarkar, 2008), *MASS* (Venables & Ripley, 2002), and *permute* (Simpson, 2022). Variables were log-transformed where necessary to fit model assumptions. We calculated Hedge's G (Cohen, 1988) using the *effect size* package (Torchiano, 2020) to compare the effects of warming treatment and season on biotic and abiotic soil properties; we considered drivers to have a significant effect when the 90% confidence intervals surrounding the effect size estimate did not overlap zero (Figure 2). We elected to use an alpha of 0.1 (and 90% confidence intervals) rather than 0.05 (or 95% confidence intervals) because we were limited by the number of field replicates we could collect and a power analysis using means for microbial biomass, soil C stocks, and extracellular enzyme data collected from the site in 2014 (Pold et al., 2017) indicated this would be needed to detect changes in mean values of 25% with a power of 80%. Figures were made using the *ggplot2* package (Wickham, 2016).

## 2.12 | Structural equation modeling

We used structural equation modeling (SEM) to test the hypothesis that long-term warming affects microbial CUE and temperature sensitivity of respiration via changes in C quantity and quality. The hypothesized path structure for the temperature sensitivity of respiration was based on the premise that long-term warming, season and soil depth had direct effects on C quantity, quality and microbial communities (fungal: bacterial ratio). These variables are then hypothesized to affect the size and temperature sensitivity of the extracellular enzyme pool and the composition of the water-extractable SOM. Finally, we hypothesized that the temperature sensitivity of respiration would be controlled by the enzyme pool, the enzyme temperature sensitivity, and the quantity and quality of soil C (Figure S8). We also completed SEM analysis on microbial CUE at 20°C. This model had a similar overall layout of the temperature sensitivity of respiration model, except that we additionally hypothesized that diversity of EcoPlate substrate consumption would be affected by season and carbon quality, and that respiration and growth would be impacted by carbon quantity and quality (Figure S9).

The SEM model path fit was performed using the *piecewiseSEM* package (Lefcheck, 2016). Cumulative enzyme activity and temperature sensitivity are represented in the model as composite variables (Lefcheck, 2016), using the mean of BG, NAG, and oxidative enzymes for the former and BG alone for the latter. We kept the model that explained the most variation in temperature sensitivity of respiration and CUE, and had a non-significant Chi-squared test ( $p > .05$ ), low Akaike information criterion (AIC) and high Comparative Fit Index (CFI > .9). If the test of direct separation (Lefcheck, 2016) identified missing paths in our hypothesized model we added these paths into the model.

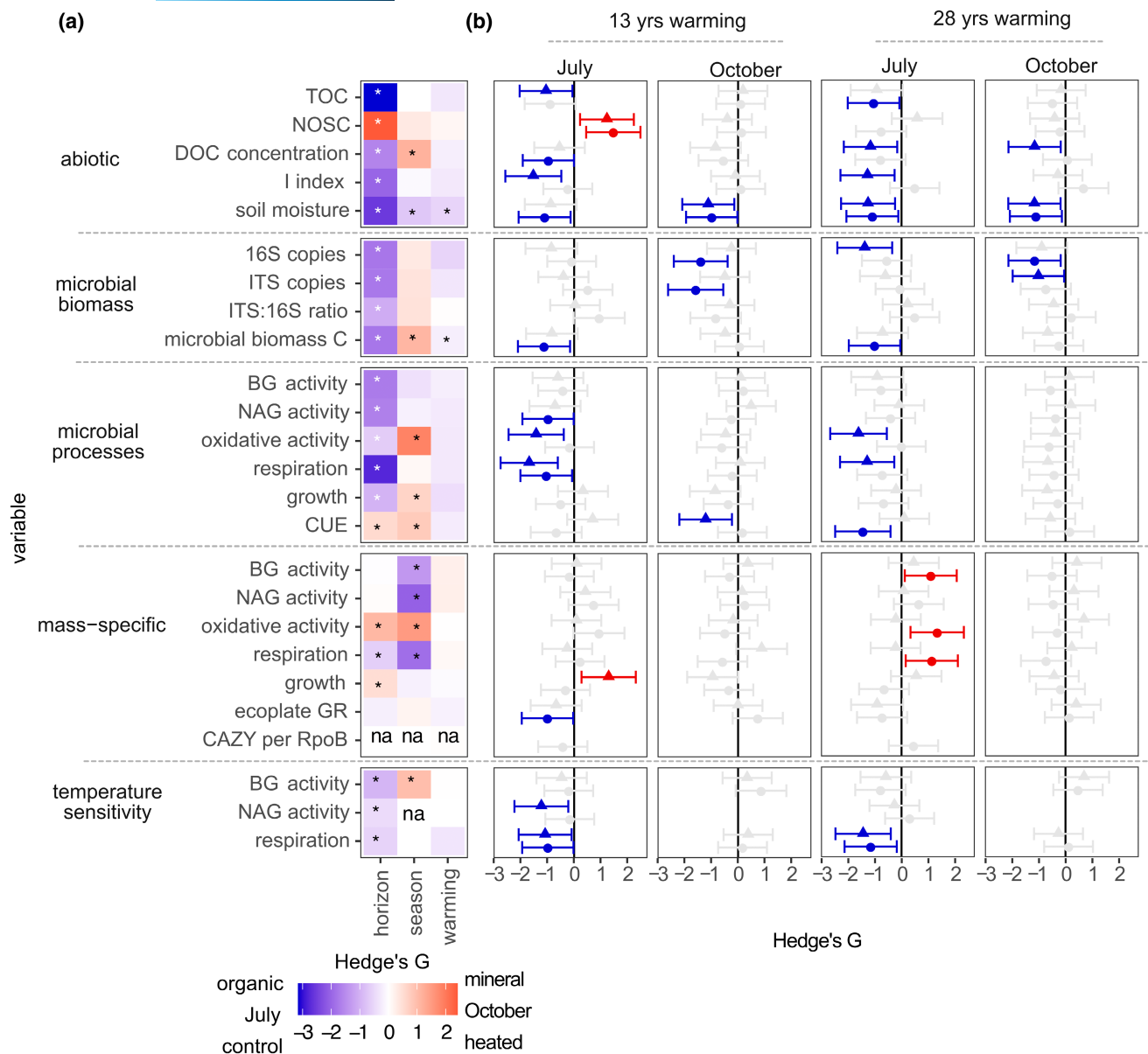


**FIGURE 2** Relative effect of experimental variables on abiotic conditions and microbial physiology. The variables surveyed were soil properties, measurements of microbial biomass, microbial activity, mass-specific microbial activity, and the temperature sensitivity of microbial activity. The heatmap shows overall differences between horizons, sampling seasons, and warming treatments (a), while the effect size plots show the effect of warming treatment within a warming experiment and sampling season (b). Blue symbols indicate a decrease with warming, red symbols an increase, and grey symbols show no warming-induced difference, based on the 90% confidence interval of Hedge's G overlapping zero. Asterisks in the heatmap similarly indicates that the 90% confidence interval does not overlap with zero.

### 3 | RESULTS

#### 3.1 | Long-term warming seasonally affects soil C substrates

Warming reduced SOM quality and quantity by most measures, but this effect was principally visible during the July sampling (Figure 2). We evaluated the chemistry of soil DOM by analyzing the polar water-extractable fraction of soil organic matter (WEOM) using metabolomics, and the thermostability of SOM using rock-eval®.

The nominal oxidation state of compounds (NOSCs) identified in the WEOM varied from -1.5 to 3, although the mean value was less than zero for all samples (Figure S7). The effect of warming on NOSC was site and time point dependent, only increasing with warming in SWaN plots in July (Figure 2, Figure S7). Warming and sampling time point did not affect the molecular complexity of the WEOM, but it was greater in mineral compared to organic soil (Figure 2a, Figure S7, mean of 143 vs 135). Overall dissimilarity in WEOM composition was primarily explained by horizon (Adonis  $R^2 = .46$ ; ADONIS  $F(1,78) = 87.50$ ,  $p < .001$ ), followed by warming treatment

(Adonis  $R^2 = .083$ ;  $F(2,78) = 7.82$ ,  $p < .001$ ) and time point (Adonis  $R^2 = .045$ ;  $F(1,78) = 8.46$ ,  $p < .001$ ). There were no significant interactions between these variables, and no evidence of heterogeneous group dispersions (i.e.,  $\text{betadisper } p > .05$ ).

Long-term warming reduced the total dissolved organic carbon in the mineral soil at the 28-year-old warming experiment at both time points, and reduced the lability index of the total SOM pool in July in both field experiments (Figure 2). Warming explained just 2.2% of the variation in SOM chemical composition based on ramped thermal rock-eval® ( $F(1,76) = 7.30$ ,  $p = .006$ ), with much of the remaining variation explained by soil horizon (Adonis  $R^2 = .71$ ,  $F(1,76) = 231.22$ ,  $p < .001$ ) and, to a lesser degree, season ( $R^2 = .020$ ,  $F(1,76) = 6.76$ ,  $p = .008$ ) (Figure 2). However, the effect of warming depended on horizon (warming  $\times$  horizon interaction  $R^2 = .011$ ,  $F(1,76) = 3.76$ ,  $p = .04$ ) and sampling time point (sampling  $\times$  warming interaction  $R^2 = .008$ ,  $F(1,76) = 2.70$ ,  $p = .09$ ). The first axis of this ordination was strongly positively correlated with the thermal labile SOM (I index) ( $\text{cor} = 0.89$ ,  $p < .001$ ).

### 3.2 | Long-term warming affects microbial communities and activity

Effects of warming on microbial communities and activity were most apparent in July (Figure 2). MBC was reduced by up to 45% in July (Figure 2a and Figure S1). Warming also reduced the July respiration at 20°C in mineral soils at both field experiments, and in organic soil samples taken from the 13-year old field experiment (Figure 2). Oxidative enzyme activity per gram of soil was also reduced by warming in the mineral soil of both sites in July, but oxidative and BG enzyme activities per unit microbial biomass were enhanced by warming in organic soils of the older field experiment (Figure 2b). Based on cultivation in EcoPlates, potential growth rate of microbial communities was unaffected by warming, except for a reduction in the organic horizon of the 13-year-old site in July (Figure 2b).

To understand how microbial communities might adapt to long-term warming in these soils we measured the temperature response of select microbial processes between 4 and 30°C. We only observed the expected increases in process rates with incubation temperature for respiration and extracellular enzyme activity (Figure 3a,b; Figures S4–S6). The temperature sensitivity of respiration was reduced by long-term warming in July in both long-term warming experiments and soil horizons (Figures 2, 3a and Figure S5).

The large variation in the  $^{18}\text{O}$  signal detected in DNA meant that growth and CUE data did not fit the expected unimodal or monotonic decline pattern, and we were unable to fit quadratic curves to the data to assess subtle shifts in the temperature optimum of growth or CUE (Figure S4). However, median CUE was greatest at 15°C across July samples and 15 or 20°C in October samples (Figure S4).

### 3.3 | Microbial activity reflects SOM chemistry

We used correlations between microbial activity per unit microbial biomass and soil properties to evaluate changes in microbial physiology. This allowed us to evaluate how processes rate and temperature sensitivity of microbial activity are associated with SOM chemistry (Figure 4). The temperature sensitivity of microbial activity was generally positively correlated with the concentration of total and dissolved SOM, and the thermal lability of SOM (I index), and negatively correlated with the NOSC and chemical complexity of WEOM (Figure 5a). Microbial biomass-specific respiration rate at 20°C showed similar correlations to SOM indices as the temperature sensitivity, but the biomass-specific rates of BG activity showed contrasting patterns. Additionally, mass-specific oxidative enzyme activity was greatest in soils characterized by chemically complex and high NOSC WEOM and with low SOM lability indices (Figure 5a). We also observed a significant positive correlation between the temperature sensitivity of respiration and the temperature sensitivity of BG activity (Figure 5b), indicating that soils with a pool of cellulolytic enzymes capable of responding to increasing temperatures also respired more in response to changing temperatures.

### 3.4 | Effects of warming on microbial physiology play out through its effects on soil C

We used path analysis to integrate the relationships between the abiotic and biotic measurements performed here and test the hypothesis that long-term warming drives microbial activity through its effect on soil C. The path analysis confirms this hypothesis and shows that long-term warming treatment, season and soil horizons influenced the carbon quantity and quality in the soil while also affecting respiration temperature sensitivity (Figure 6). However, long-term warming duration has no direct effect on microbial physiology or WEOM and SOM quality. Unexpectedly, the nominal oxidation state of water-extractable organic matter was not a key integrator of shifts in SOM chemistry and did not drive respiration temperature sensitivity (Figure 6). Rather, temperature sensitivity of respiration was directly correlated with quantity of carbon and the size of the extracellular enzyme pool and temperature sensitivity of BG.

Season had a direct effect on the dissolved fraction of SOM and C quality while increasing soil depth decreased the SOM quality (e.g., labile fraction). Respiration temperature sensitivity was driven directly by the enzyme pool in soils, carbon quantity and the enzyme temperature sensitivity. The soil potential extracellular enzyme activity was driven by C quantity and season while the enzyme temperature sensitivity was driven by both season and carbon quantity. Although microbial communities can modulate thermal acclimation, the fungal to bacterial ratio was only driven by soil horizon and did not influence other parameters in our model. Our SEM model explained 27% of the variance in the temperature sensitivity of

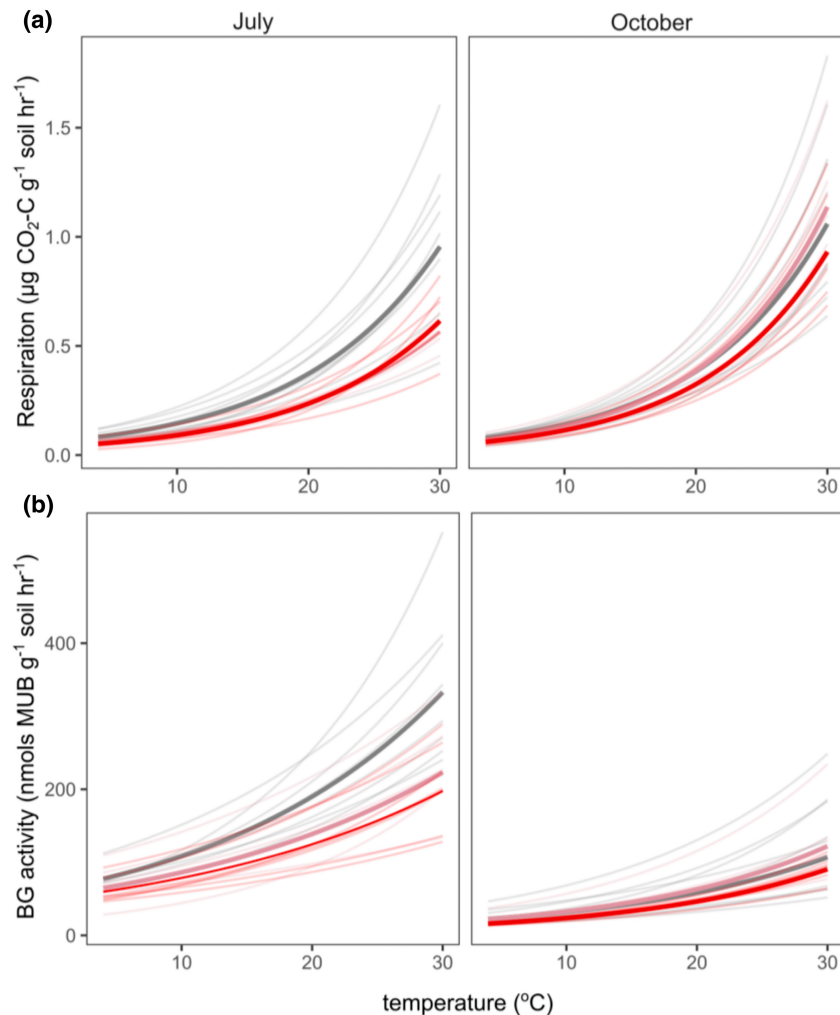


**FIGURE 3** Temperature sensitivity of microbial carbon cycling processes. Respiration rate (a) and BG extracellular enzyme activity (b) at different temperatures from 4 to 30°C measured under laboratory incubations in July and October for the mineral soils. Thin lines correspond to Taylor exponential model fit to individual samples and thick lines the overall fit to all replicates of a treatment. Grey corresponds to control plots, pink to 13 years of warming (SWaN) and red to 28 years of warming (PH).

respiration, although many of the drivers of temperature sensitivity were explained to a much greater degree.

Path analysis shows that CUE at 20°C is directly affected by respiration and growth as expected, but also by other factors such as the dissolved SOM fraction and season, with higher CUE measured in October compared to July (Figure 7, Figure S4). The mass-specific microbial respiration component of CUE was much better explained than the growth component ( $R^2 = .77$  vs.  $.14$ ), with 86% of the variation in CUE explained overall (Figure 7). This was expected given the large variation in our measurements of growth rate. Distinct factors also drove respiration and growth differently. The mass-specific enzyme pool only drives respiration while carbon quality correlates positively with mass-specific respiration and negatively with mass-specific growth.

In order to avoid the potential problems associated with predicting CUE from its constituent components (i.e., growth and respiration), we also built a SEM without these variables to evaluate how much the other variables we measured directly explained CUE (Figure S10). This model captures 39% of CUE variance and the direct drivers were season, mass-specific enzyme pool, and carbon quality. High-quality carbon is associated with lower CUE in both models because it accelerates mass-specific respiration while slowing mass-specific growth (Figure 7 and Figure S10).

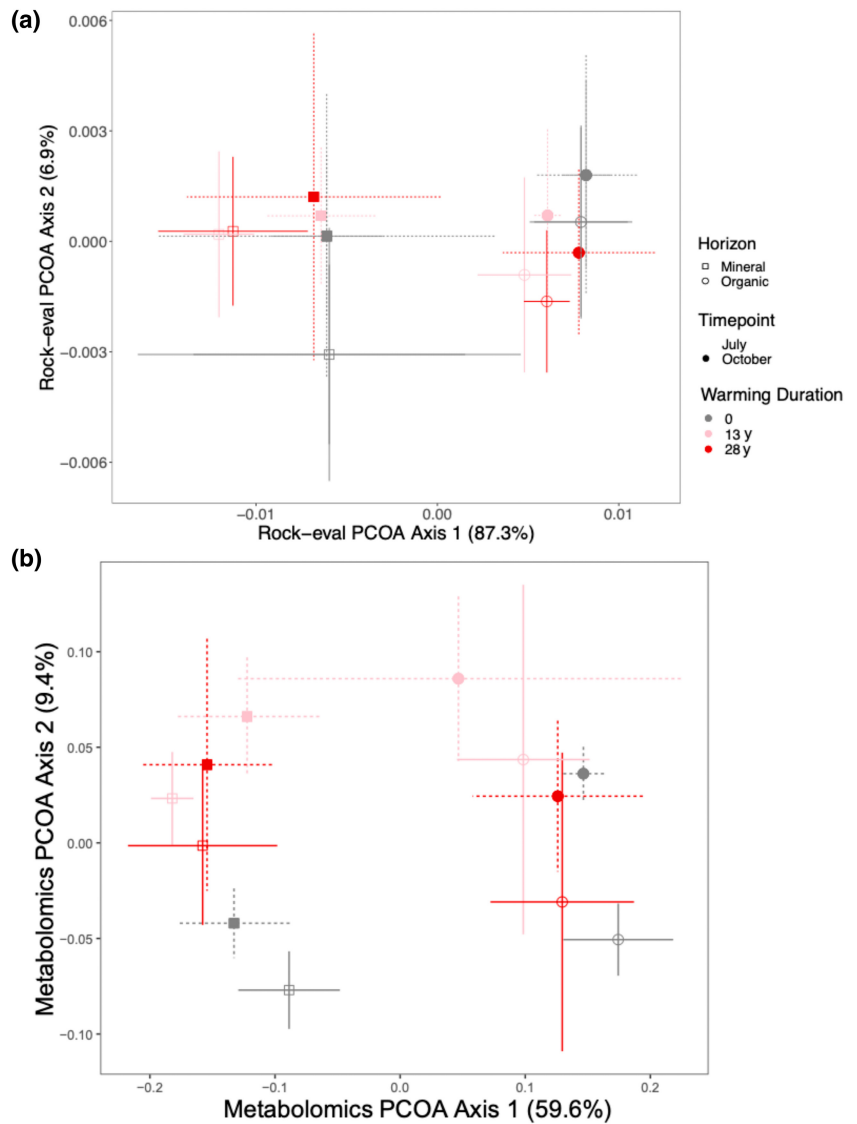
## 4 | DISCUSSION

### 4.1 | Long-term warming impact on SOM chemistry

Here, we evaluated the hypothesis that the effect of warming on microbial physiology plays out through its effects on the quantity and quality of SOM. We found that while soil chemistry had predictable correlations with microbial activity, the effects of warming on SOM chemistry—and, in turn, microbial physiology—were mostly limited to summer. Therefore, the effect of warming on microbial physiology depends on its effects on SOM chemistry.

The effect of warming on SOM quality was most apparent in the mineral soil, where soil lability index was reduced (Figure 2b). This is consistent with previous studies at these sites which show that warming-associated changes in soil organic matter quality are especially apparent in the mineral soil and typical plant-derived compounds such as lignin and polysaccharides were more depleted after 4 and 23 years of warming (Pisani et al., 2015; Pold et al., 2017). Greater decomposition with warming has also increased overall relative abundance of lipids (Pec et al., 2021; Pisani et al., 2015; Pold et al., 2017; VandenEnden et al., 2021) despite a reduction in plant lipids (Pisani

**FIGURE 4** Soil organic matter quality. Ordination of soil organic matter composition from control and heated soils differing in warming duration (13 or 28 years) sampled in July and October and different soils depths (mineral and organic) based on principal coordinate analysis (PCOA) from the pyrolyzed fraction of SOM based on rock-eval® (a) and water-extractable polar metabolites (b).



et al., 2015), indicating further microbial processing. Lignin and lipids are both among the least oxidized (LaRowe & Van Cappellen, 2011) and most readily pyrolyzed (Sanderman & Grandy, 2020) compounds found in soil, such that a potential shift toward being more lipid-rich and lignin-poor SOM under warming in the organic soil would not be detected. However, it is more probable that any signal of increased microbial processing was drowned out in the high plant input: microbial processing ratio in the organic soil. This is consistent with the observation that warming does not consistently alter SOM quality throughout seasons, even in the more microbial necromass-dominated mineral soil (Figure 2b and Figure S1). Rather, differences were only apparent in our summer sampling when belowground inputs likely dominated carbon inputs (Abramoff & Finzi, 2015; Cheeke et al., 2021), and not following the autumn leaf litter influx. This is consistent with a wealth of studies indicating that season strongly regulates the input of plant material and nutrients in temperate forest soils and that this seasonality is associated with variation in microbial activity and biomass (Cheeke et al., 2021; Kaiser et al., 2010; Pold et al., 2017; Rasche et al., 2011; Wardle et al., 2004).

#### 4.2 | SOM chemistry impact on microbial thermal acclimation, biomass, and activity

The seasonal dependence of warming effects on SOM chemistry was further associated with temporally inconsistent effects of warming on microbial physiology. Limited substrate availability has been cited as necessary condition for microbial community physiological acclimation under warming (Alster et al., 2022; Bradford, 2013; Fierer et al., 2006; Kirschbaum, 2004; Luo et al., 2001; Moinet et al., 2021). We only observed apparent thermal acclimation of C cycling processes when the input of fresh plant material was limited (i.e., in summer), and not once a pulse of fresh aboveground plant input reaches the soil (i.e., in autumn; Figures 2b and 3). Temperature is an important driver controlling how soil microbes degrade organic matter (Bradford, 2013), and to a certain degree elevated temperatures may help microbes overcome substrate limitation by accelerating the rate at which extracellular enzymes process SOM. However, as warmer temperatures sustain accelerated microbial activity through time, substrates ultimately become depleted and the temporary warming-induced increase in respiration ceases

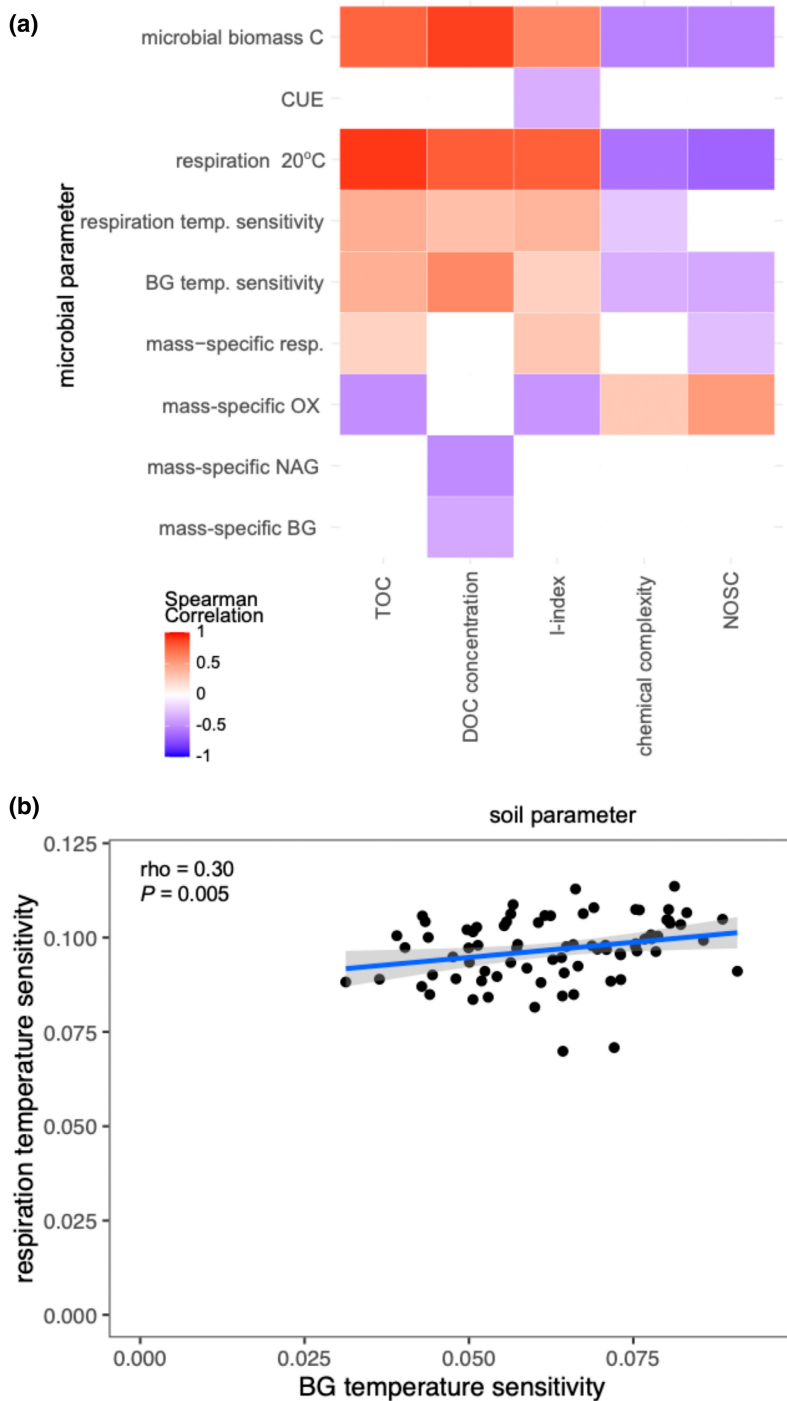


**FIGURE 5** Relationship between the quantity and quality of soil organic matter and the response of microbial physiology. Heat map of soil parameters and microbial physiology measurements across all samples (a), TOC: Total carbon quantified during rock-eval® ramped thermal pyrolysis, DOC concentration: Dissolved fraction of organic carbon measured by a TOC-L analyzer; l-index: Thermal labile SOM fraction based on rock-eval®, chemical complexity: Based on polar metabolites; "NOSC": Mean nominal oxidation state based on polar metabolites, and relationship between the temperature sensitivity of respiration and extracellular enzymatic activity (b). Spearman correlation coefficients in (a) are shown as white where the Benjamini-Hochberg corrected  $p$ -value exceeded .05.

(Luo et al., 2001; Romero-Olivares et al., 2017; Walker et al., 2018). This substrate depletion leads to a reduction in microbial biomass followed by a decrease in microbial activity (Walker et al., 2018). However, as seen here, seasonal flushes of fresh aboveground litter inputs may temporarily mitigate this warming-induced substrate depletion, allowing microbial biomass and therefore process rates to somewhat recover to the levels observed in the absence of chronic warming. This concept of substrate limitation induced reductions in microbial activity via reductions in microbial biomass is supported by the observation that biomass-specific C processes rates are less affected by warming compared to the activities measured on a per gram

of soil basis (Figure 2b). Accordingly, two metrics strongly correlated with microbial biomass—total organic carbon and size of the extracellular enzymatic pool—along with temperature sensitivity of extracellular enzyme activity, were the main drivers of respiration temperature sensitivity (Figure 6).

Part of the greater respiration temperature sensitivity with larger enzyme pools may be linked to greater temperature sensitivity of extracellular enzyme activity, enabling greater supply rate of products for microbial metabolism without greater investment in those enzymes. However, the connection between the temperature sensitivity of respiration and extracellular enzyme activity is not

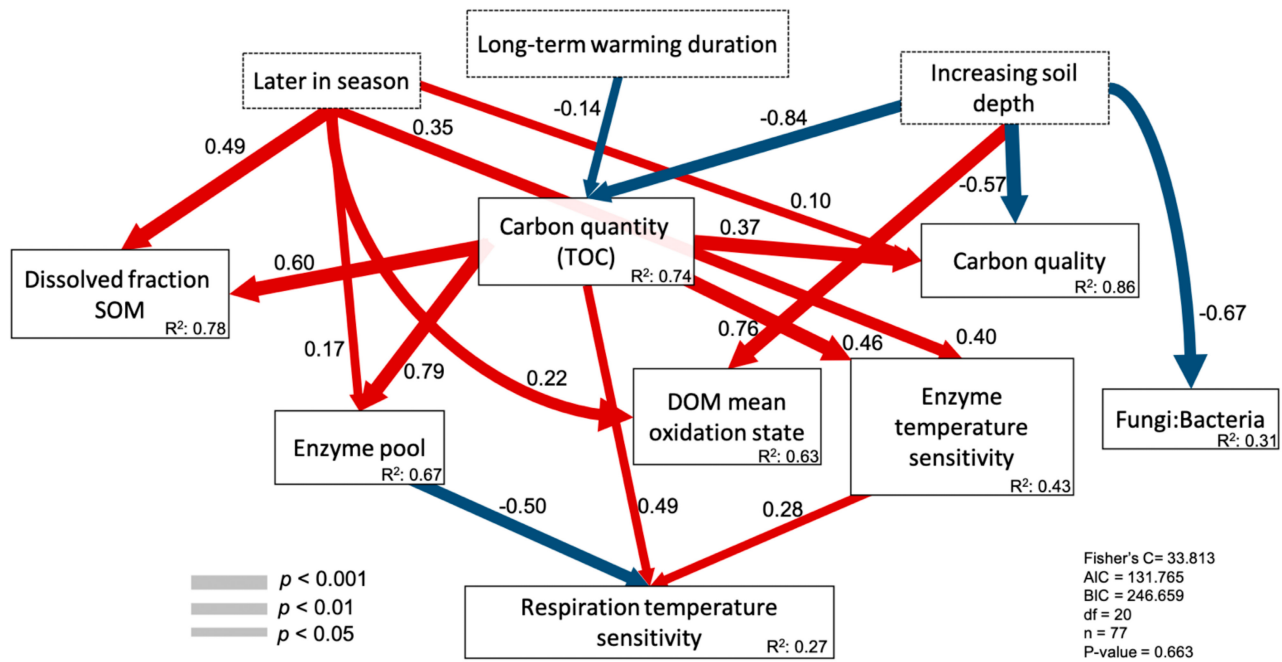


**FIGURE 6** Structural equation model showing the relative influence of long-term warming duration, soil horizons and different seasons (October and July) on abiotic factors and components of microbial physiology driving the respiration temperature sensitivity. Significant paths are shown in red if positive or in blue if negative. Path width corresponds to degree of significance as shown in the lower left. The amount of variance explained by the model ( $R^2$ ) is shown for each response variable, and measures of overall model fit are shown in the lower right. Dissolved fraction of SOM: Dissolved organic carbon measured by a TOC-L analyzer; carbon quantity: Total carbon quantified during rock-eval® ramped thermal pyrolysis; carbon quality: PCOA axis 1 of rock-eval® ramped thermal pyrolysis; enzyme pool: Composite variable of maximum activity recorded for BG, NAG, and oxidative enzymes; WEOM mean oxidation state: SOM oxidation state calculated from polar metabolites; enzyme temperature sensitivity: BG activity response to temperature while incubated from 4 to 30°C; fungi:Bacteria: 16S rRNA gene copy number  $g^{-1}$  soil: ITS gene copy number  $g^{-1}$  soil; respiration temperature sensitivity: Respiration response to temperature while incubated from 4 to 30°C. Global goodness-of-fit: Fisher's C.

equally linked to all SOM pools equally; soil samples with a bigger pool of cellulolytic enzymes were more capable of responding to increasing temperatures and consequently respired more in response to changing temperatures (Figure 6). Therefore, our results implicate the relevance of SOM quantity in driving microbial community activity (Kirschbaum, 2004; Moinet et al., 2021) and functioning (Domeignoz-Horta et al., 2021).

### 4.3 | Relationships between SOM quantity and quality to microbial CUE

Carbon use efficiency is an important integrator of C quality with microbial metabolism, both because of the costs associated with extracellular enzyme production necessary to access those substrates (Domeignoz-Horta et al., 2020; Malik et al., 2019), and because of differences in the communities able to use and the energetic yield associated with the use of those different substrates (Pold, Domeignoz-Horta, Morrison, et al., 2020). The respiration component of CUE was more responsive to changes in SOM and WEOM pools compared to growth, indicating that growth has a relatively fixed cost compared to respiration. This is in line with the observation that microbes may downregulate the protein production machinery in response to warming-induced substrate

depletion, allowing them to sustain growth (Sollinger et al., 2022) while the respiration component could then absorb changes in substrate quantity and quality. This downregulation of the protein machinery does not require a change in the active community (Sollinger et al., 2022). Changes in the microbial community have historically been variable and limited at our study sites (DeAngelis et al., 2015; Frey et al., 2008; Pec et al., 2021; Roy Chowdhury et al., 2021), and we did not observe a change in the F:B ratio under warming here (Figure S3). Nor did we observe a correlation between F:B ratio and CUE. This reinforces the idea that substrates quality and quantity rather than microbial identity have the dominant effect on CUE and its response to long-term warming in these soils (Figures 5, 7 and Figure S10).

Microbial activity measurements are more strongly correlated with the thermal lability (l index) of the total organic matter measured by rock-eval® than the water-extractable pool measured by polar metabolomics. It is uncertain whether this is due to the latter method missing the compounds most important for microbial activity over the course of the assays period, or whether the chemistry of bulk SOM rather than the water-extractable component is truly a better predictor of microbial physiology. Nonetheless, our results show that SOM thermal-lability index based on rock-eval® captures organic matter pools which vary between soils characterized by divergent microbial community metabolisms. The warming

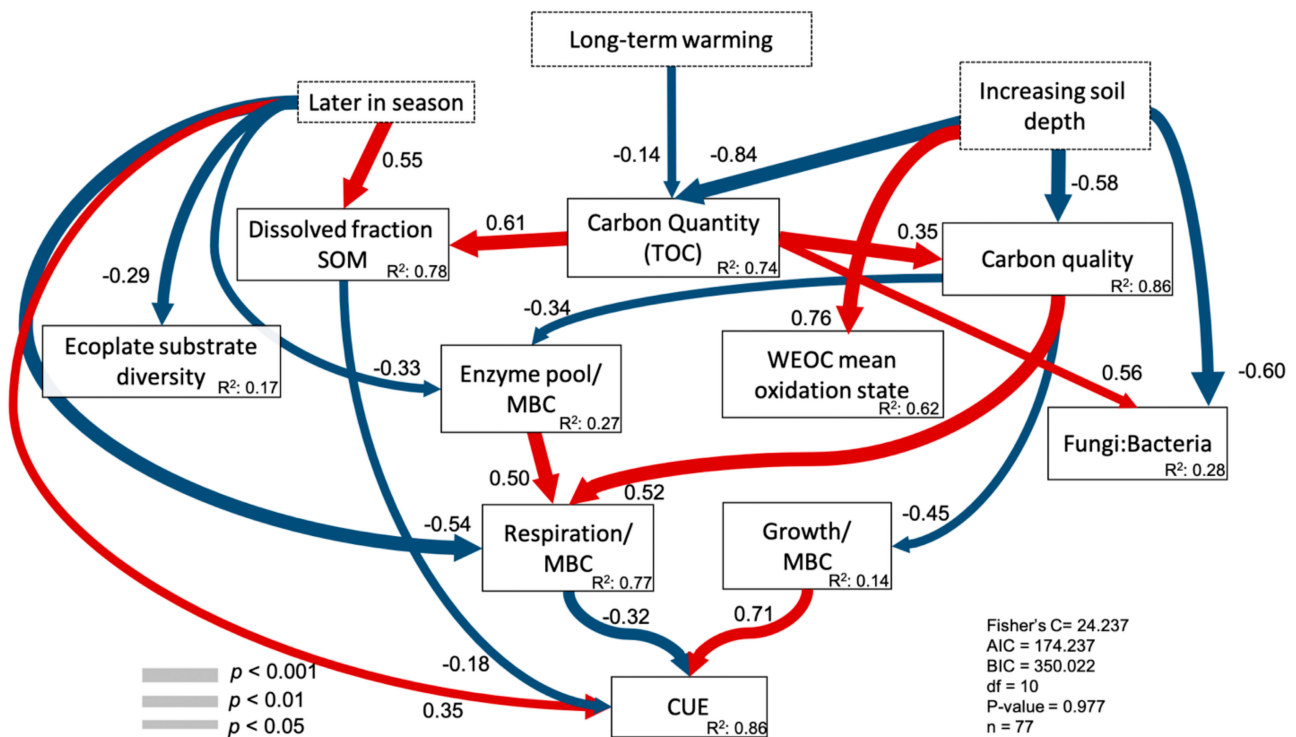


**FIGURE 7** Structural equation model showing the relative influence of long-term warming duration, soil horizons and different seasons (October and July) on abiotic factors and components of microbial physiology driving CUE. Significant paths are shown in red if positive or in blue if negative. Path width corresponds to degree of significance as shown in the lower left. The amount of variance explained by the model ( $R^2$ ) is shown for each response variable, and measures of overall model fit are shown in the lower right. Dissolved fraction of SOM: Dissolved organic carbon measured by a TOC-L analyzer; carbon quantity: Total carbon quantified during rock-eval® ramped thermal pyrolysis; carbon quality: PCOA axis 1 of rock-eval® ramped thermal pyrolysis; enzyme pool/MBC: Composite variable of maximum activity recorded for BG, NAG, and oxidative enzymes by microbial biomass carbon; SOM mean oxidation state: SOM oxidation state calculated from polar metabolites; fungi:Bacteria: 16S rRNA gene copy number  $g^{-1}$  soil; ITS gene copy number  $g^{-1}$  soil; respiration/MBC: Respiration measured at 20°C/microbial biomass carbon; growth/MBC: Growth measured at 20°C/microbial biomass carbon and CUE: Carbon use efficiency measured at 20°C; global goodness-of-fit: Fisher's C.

impact on resource availability is inconsistent due to seasonality in inputs (Figures 2 and 3), which might result in a variable selection regime (McDonald, 2019) limiting the degree of intrinsic thermal acclimation of the microbial community to long-term warming in these soils. As such, our results are consistent with previous findings that the response of microbial communities to global warming and its potential impact on soil carbon stocks will depend on concurrent changes in soil organic matter chemistry and availability to microorganisms (Bradford et al., 2008; Melillo et al., 2017). While we still lack a clear understanding of the controls that drive variation in the response of soil carbon to warmer temperatures globally (Van Gestel et al., 2018), our results identify the direct drivers of apparent thermal acclimation of C processes drawing attention to the importance to monitor soil C chemistry to better understand possible soil C feedback mechanisms to the atmosphere as the world warms.

## 5 | CONCLUSION

Here, we evaluated the interplay between the biotic and abiotic components of an ecosystem exposed to long-term warming to

understand the mechanisms underlying the microbial physiological response to warming. We recorded that the apparent thermal acclimation of respiration and extracellular enzyme activities in heated soils compared to control soils in the summer sampling was caused by lower substrate availability due to long-term warming. We did not detect an effect of long-term warming on the temperature sensitivity of any C-cycling process in autumn, which we propose is due to litter deposition alleviating summer substrate depletion. By disentangling the direct drivers of apparent thermal acclimation in long-term warmed soils these results highlight that improved quantitative predictions of soil C stocks under warming requires considering concurrent qualitative changes in SOM quality.

## AUTHOR CONTRIBUTIONS

Grace Pold, Luiz A. Domeignoz-Horta, and Kristen M. DeAngelis designed the laboratory experiments. Serita D. Frey and Jerry M. Melillo designed the field experiments. Grace Pold, Luiz A. Domeignoz-Horta, Melissa A. Knorr, and Hailey Erb conducted the experiments. Luiz A. Domeignoz-Horta, Grace Pold, D.S. and Katherine Louie analyzed the data. Luiz A. Domeignoz-Horta and Grace Pold wrote the first draft of the paper. Grace Pold, Luiz A. Domeignoz-Horta,

Kristen M. DeAngelis, Serita D. Frey, Jerry M. Melillo, David Sebag, Katherine Louie, Eric Verrecchia, Hailey Erb, Trent Northen, Emiley Eloie-Fadrosch, Christa Pennacchio, and Melissa A. Knorr contributed to revising the manuscript.

**ACKNOWLEDGMENTS**

The authors thank Achala Narayanan, Xiao-Jun Allen Liu, and Melisa Shinfuku for helping with samples processing. Funding for this project was provided by the National Science Foundation (NSF)(DEB-1749206) to K.M.D.; NSF Long-Term Research in Environmental Biology (DEB-1456528) to K.M.D., S.D.F., and J.M.M.; and NSF Long-Term Ecological Research (DEB-1832210) programs. This work was also conducted with support (proposal 506489: 10.46936/10.25585/60001340 to L.A.D.-H. and K.M.D.) from the U.S. Department of Energy Joint Genome Institute (<https://ror.org/04xm1d337>), a DOE Office of Science User Facility, is supported by the Office of Science of the U.S. Department of Energy operated under Contract No. DE-AC02-05CH11231.

**CONFLICT OF INTEREST**

The authors declare no competing interests.

**DATA AVAILABILITY STATEMENT**

Metagenomes generated during this study are available at the JGI Gold portal with the ID Gs0149985 (Table S2). All data and codes used in this study can be obtained in the Dryad platform (<https://doi.org/10.5061/dryad.sxksn036t>) or Open Science Framework Project (<https://osf.io/zdhfb/>), from the supplementary materials (Tables S3-S6) and from the authors upon request.

**ORCID**

- Luiz A. Domeignoz-Horta  <https://orcid.org/0000-0003-4618-6253>
- Grace Pold  <https://orcid.org/0000-0003-4418-4246>
- Hailey Erb  <https://orcid.org/0000-0003-3729-5634>
- David Sebag  <https://orcid.org/0000-0002-6446-6921>
- Katherine Louie  <https://orcid.org/0000-0002-6787-7558>
- Emiley Eloie-Fadrosch  <https://orcid.org/0000-0002-8162-1276>
- Serita D. Frey  <https://orcid.org/0000-0002-9221-5919>
- Kristen M. DeAngelis  <https://orcid.org/0000-0002-5585-4551>

**REFERENCES**

Abramoff, R. Z., & Finzi, A. C. (2015). Are above-and below-ground phenology in sync? *New Phytologist*, 205(3), 1054–1061.

Allison, S. D., Romero-Olivares, A. L., Lu, Y., Taylor, J. W., & Treseder, K. K. (2018). Temperature sensitivities of extracellular enzyme v<sub>max</sub> and k<sub>m</sub> across thermal environments. *Global Change Biology*, 24(7), 2884–2897.

Allison, S. D., Wallenstein, M. D., & Bradford, M. A. (2010). Soil-carbon response to warming dependent on microbial physiology. *Nature Geoscience*, 3(5), 336–340.

Alster, C. J., Robinson, J. M., Arcus, V. L., & Schipper, L. A. (2022). Assessing thermal acclimation of soil microbial respiration using macromolecular rate theory. *Biogeochemistry*, 158, 1–11.

Berlemont, R., Martiny, A. C., & Kivisaar, M. (2015). Genomic potential for polysaccharide deconstruction in bacteria. *Applied and Environmental Microbiology*, 81(4), 1513–1519. <https://doi.org/10.1128/AEM.03718-14>

Bolan, N. S., Adriano, D. C., Kunhikrishnan, A., James, T., McDowell, R., & Senesi, N. (2011). Dissolved organic matter: Biogeochemistry, dynamics, and environmental significance in soils. *Advances in Agronomy*, 110, 1–75.

Bölscher, T., Ågren, G. I., & Herrmann, A. M. (2020). Land-use alters the temperature response of microbial carbon-use efficiency in soils—A consumption-based approach. *Soil Biology and Biochemistry*, 140, 107639. <https://doi.org/10.1016/j.soilbio.2019.107639>

Bradford, M. A. (2013). Thermal adaptation of decomposer communities in warming soils. *Frontiers in Microbiology*, 4, 333.

Bradford, M. A., Davies, C. A., Frey, S. D., Maddox, T. R., Melillo, J. M., Mohan, J. E., Reynolds, J. F., Treseder, K. K., & Wallenstein, M. D. (2008). Thermal adaptation of soil microbial respiration to elevated temperature. *Ecology Letters*, 11(12), 1316–1327.

Burns, R. G., & Dick, R. P. (Eds.). (2002). *Enzymes in the environment: Activity, ecology, and applications*. CRC Press.

Carey, J. C., Tang, J., Templer, P. H., Kroeger, K. D., Crowther, T. W., Burton, A. J., Dukes, J. S., Emmett, B., Frey, S. D., Heskell, M. A., Jiang, L., Machmuller, M. B., Mohan, J., Panetta, A. M., Reich, P. B., Reinsch, S., Wang, X., Allison, S. D., Bamminger, C., ... Tietema, A. (2016). Temperature response of soil respiration largely unaltered with experimental warming. *Proceedings of the National Academy of Sciences of the USA*, 113(48), 13797–13802.

Cavicchioli, R., Ripple, W. J., Timmis, K. N., Azam, F., Bakken, L. R., Baylis, M., Behrenfeld, M. J., Boetius, A., Boyd, P. W., Classen, A. T., Crowther, T. W., Danovaro, R., Foreman, C. M., Huisman, J., Hutchins, D. A., Jansson, J. K., Karl, D. M., Koskella, B., Mark Welch, D. B., ... Webster, N. S. (2019). Scientists' warning to humanity: Microorganisms and climate change. *Nature Reviews Microbiology*, 17, 569–586. <https://doi.org/10.1038/s41579-019-0222-5>

Cheeke, T. E., Phillips, R. P., Kuhn, A., Rösling, A., & Fransson, P. (2021). Variation in hyphal production rather than turnover regulates standing fungal biomass in temperate hardwood forests. *Ecology*, 102(3), e03260.

Cohen, J. (1988). *Statistical power analysis for the behavioral sciences* (2nd ed.). Lawrence Erlbaum Associates. <https://doi.org/10.4324/9780203771587>

Contosta, A. R., Frey, S. D., & Cooper, A. B. (2011). Seasonal dynamics of soil respiration and n mineralization in chronically warmed and fertilized soils. *Ecosphere*, 2(3), 1–21.

Davidson, E. A., & Janssens, I. A. (2006). Temperature sensitivity of soil carbon decomposition and feedbacks to climate change. *Nature*, 440(7081), 165–173. <https://doi.org/10.1038/nature04514>

DeAngelis, K. M., Pold, G., Topçuoğlu, B. D., van Diepen, L. T. A., Varney, R. M., Blanchard, J. L., & Frey, S. D. (2015). Long-term forest soil warming alters microbial communities in temperate forest soils. *Frontiers in Microbiology*, 6, 104.

Domeignoz-Horta, L. A., Pold, G., Liu, X. J. A., Frey, S. D., Melillo, J. M., & DeAngelis, K. M. (2020). Microbial diversity drives carbon use efficiency in a model soil. *Nature Communications*, 11(1), 1–10. <https://doi.org/10.1038/s41467-020-17502-z>

Domeignoz-Horta, L. A., Shinfuku, M., Junier, P., Poirier, S., Verrecchia, E., Sebag, D., & DeAngelis, K. M. (2021). Direct evidence for the role of microbial community composition in the formation of soil organic matter composition and persistence. *ISME Communications*, 1(1), 64. <https://doi.org/10.1038/s43705-021-00071-7>

Feng, X., Simpson, A. J., Wilson, K. P., Williams, D. D., & Simpson, M. J. (2008). Increased cuticular carbon sequestration and lignin oxidation in response to soil warming. *Nature Geoscience*, 1(12), 836–839.

- Fierer, N., Colman, B. P., Schimel, J. P., & Jackson, R. B. (2006). Predicting the temperature dependence of microbial respiration in soil: A continental-scale analysis. *Global Biogeochemical Cycles*, 20(3), GB3026. <https://doi.org/10.1029/2005GB002644>
- Fierer, N., Jackson, J. A., Vilgalys, R., & Jackson, R. B. (2005). Assessment of soil microbial community structure by use of taxon-specific quantitative PCR assays. *Applied Environmental Microbiology*, 71(7), 4117–4120.
- Frey, S., Drijber, R., Smith, H., & Melillo, J. (2008). Microbial biomass, functional capacity, and community structure after 12 years of soil warming. *Soil Biology and Biochemistry*, 40(11), 2904–2907.
- Frey, S. D., Lee, J., Melillo, J. M., & Six, J. (2013). The temperature response of soil microbial efficiency and its feedback to climate. *Nature Climate Change*, 3(4), 395–398.
- German, D. P., Weintraub, M. N., Grandy, A. S., Lauber, C. L., Rinkes, Z. L., & Allison, S. D. (2011). Optimization of hydrolytic and oxidative enzyme methods for ecosystem studies. *Soil Biology and Biochemistry*, 43(7), 1387–1397.
- Gommers, P., Van Schie, B., Van Dijken, J., & Kuenen, J. (1988). Biochemical limits to microbial growth yields: An analysis of mixed substrate utilization. *Biotechnology and Bioengineering*, 32(1), 86–94.
- Gunina, A., & Kuznyakov, Y. (2022). From energy to (soil organic) matter. *Global Change Biology*, 28(7), 2169–2182. <https://doi.org/10.1111/gcb.16071>
- Hall, E. K., Singer, G. A., Kainz, M. J., & Lennon, J. T. (2010). Evidence for a temperature acclimation mechanism in bacteria: An empirical test of a membrane-mediated trade-off. *Functional Ecology*, 24(4), 898–908.
- Hartley, I. P., Heinemeyer, A., & Ineson, P. (2007). Effects of three years of soil warming and shading on the rate of soil respiration: Substrate availability and not thermal acclimation mediates observed response. *Global Change Biology*, 13(8), 1761–1770.
- Huntemann, M., Ivanova, N., Mavromatis, K., Tripp, H., Paez-Espino, D., Tennessen, K., Palaniappan, K., Szeto, E., Pillay, M., Chen, I. A., Pati, A., Nielsen, T., Markowitz, V. M., & Kyrpides, N. C. (2016). The standard operating procedure of the DOE-JGI metagenome annotation pipeline (map v. 4). *Standards in Genomic Sciences*, 11, 88.
- Kahm, M., Hasenbrink, G., Lichtenberg-Frat'e, H., Ludwig, J., & Kschischo, M. (2010). Grofit: Fitting biological growth curves with R. *Journal of Statistical Software*, 33(7), 1–21.
- Kaiser, C., Koranda, M., Kitzler, B., Fuchslueger, L., Schnecker, J., Schweiger, P., Rasche, F., Zechmeister-Boltenstern, S., Sessitsch, A., & Richter, A. (2010). Belowground carbon allocation by trees drives seasonal patterns of extracellular enzyme activities by altering microbial community composition in a beech forest soil. *New Phytologist*, 187(3), 843–858.
- Kirschbaum, M. U. (2004). Soil respiration under prolonged soil warming: Are rate reductions caused by acclimation or substrate loss? *Global Change Biology*, 10(11), 1870–1877. <https://doi.org/10.1111/j.1365-2486.2004.00852.x>
- LaRowe, D. E., & Van Cappellen, P. (2011). Degradation of natural organic matter: A thermodynamic analysis. *Geochimica et Cosmochimica Acta*, 75(8), 2030–2042.
- Lefcheck, J. S. (2016). Piecewissem: Piecewise structural equation modeling in R for ecology, evolution, and systematics. *Methods in Ecology and Evolution*, 7(5), 573–579. <https://doi.org/10.1111/2041-210X.12512>
- Liu, X. J. A., Pold, G., Domeignoz-Horta, L. A., Geyer, K. M., Caris, H., Nicolson, H., Kemner, K. M., Frey, S. D., Jerry, M. M., & DeAngelis, K. M. (2021). Soil aggregate-mediated microbial responses to long-term warming. *Soil Biology and Biochemistry*, 152, 108055.
- Lloyd, J., & Taylor, J. A. (1994). On the temperature dependence of soil respiration. *Functional Ecology*, 8(3), 315–323.
- Luo, Y., Wan, S., Hui, D., & Wallace, L. L. (2001). Acclimatization of soil respiration to warming in a tall grass prairie. *Nature*, 413(6856), 622–625. <https://doi.org/10.1038/35098065>
- Malik, A. A., Puissant, J., Goodall, T., Allison, S. D., & Griffiths, R. I. (2019). Soil microbial communities with greater investment in resource acquisition have lower growth yield. *Soil Biology and Biochemistry*, 132, 36–39. <https://doi.org/10.1016/j.soilbio.2019.01.025>
- Malik, A., & Gleixner, G. (2013). Importance of microbial soil organic matter processing in dissolved organic carbon production. *FEMS Microbiology Ecology*, 86(1), 139–148.
- McDonald, M. J. (2019). Microbial experimental evolution—A proving ground for evolutionary theory and a tool for discovery. *EMBO Reports*, 20(8), 1–14. <https://doi.org/10.15252/embr.201846992>
- Melillo, J., Steudler, P., Aber, J., Newkirk, K., Lux, H., Bowles, F., Catricala, C., Magill, A., Ahrens, T., & Morrisseau, S. (2002). Soil warming and carbon-cycle feedbacks to the climate system. *Science*, 298(5601), 2173–2176.
- Melillo, J. M., Frey, S. D., DeAngelis, K. M., Werner, W. J., Bernard, M. J., Bowles, F. P., Pold, G., Knorr, M. A., & Grandy, A. S. (2017). Long-term pattern and magnitude of soil carbon feedback to the climate system in a warming world. *Science*, 358(6359), 101–105. <https://doi.org/10.1126/science.aan2874>
- Mendiburu, F. D. (2019). *Agricolae: Statistical procedures for agricultural research* [Computer software manual]. (R package version 1.3-1).
- Moinet, G. Y., Dhami, M. K., Hunt, J. E., Podolyan, A., Liang, L. L., Schipper, L. A., Whitehead, D., Nuñez, J., Nascente, A., & Millard, P. (2021). Soil microbial sensitivity to temperature remains unchanged despite community compositional shifts along geothermal gradients. *Global Change Biology*, 27(23), 6217–6231. <https://doi.org/10.1111/gcb.15878>
- Munger, W., & Wofsy, S. (2021). Biomass inventories at Harvard forest EMS tower since 1993. *Harvard Forest Data Archive*, 37, HF069. <https://doi.org/10.6073/pasta/cd913a57d7f138b832b7f90b53ae21be>
- Muth, C. C., & Bazzaz, F. (2002). Tree canopy displacement at forest gap edges. *Canadian Journal of Forest Research*, 32(2), 247–254.
- Nyamundanda, G., Brennan, L., & Gormley, I. C. (2010). Probabilistic principal component analysis for metabolomic data. *BMC Bioinformatics*, 11(1), 1–11.
- Oksanen, J., Blanchet, F. G., Friendly, M., Kindt, R., Legendre, P., McGinn, D., Minchin, P. R., O'Hara, R. B., Simpson, G. L., Solyomos, P., Stevens, M. H. H., Szocs, E., & Wagner, H. (2019). *vegan: Community ecology package* [Computer software manual]. (R package version 2.5-4).
- Paradis, E., & Schliep, K. (2019). Ape 5.0: An environment for modern phylogenetics and evolutionary analyses in R. *Bioinformatics*, 35(3), 526–528.
- Pec, G. J., van Diepen, L. T. A., Knorr, M., Grandy, A. S., Melillo, J. M., DeAngelis, K. M., Blanchard, J. L., & Frey, S. D. (2021). Fungal community response to long-term soil warming with potential implications for soil carbon dynamics. *Ecosphere*, 12(5), e03460.
- Pinheiro, J., Bates, D., DebRoy, S., Sarkar, D., & R Core Team. (2019). *nlme: Linear and nonlinear mixed effects models* [Computer software manual]. (R package version 3.1–140).
- Pisani, O., Frey, S. D., Simpson, A. J., & Simpson, M. J. (2015). Soil warming and nitrogen deposition alter soil organic matter composition at the molecular-level. *Biogeochemistry*, 123(3), 391–409.
- Pold, G., Billings, A. F., Blanchard, J. L., Burkhardt, D. B., Frey, S. D., Melillo, J. M., Schnabel, J., van Diepen, L. T. A., & DeAngelis, K. (2016). Long-term warming alters carbohydrate degradation potential in temperate forest soils. *ASM Journals on CD*, 82(22), 6518–6530.
- Pold, G., Domeignoz-Horta, L. A., & DeAngelis, K. M. (2020). Heavy and wet: The consequences of violating assumptions of measuring soil microbial growth efficiency using the <sup>18</sup>O water method. *Elementa: Science of the Anthropocene*, 8(1), 069. <https://doi.org/10.1525/elementa.069>
- Pold, G., Domeignoz-Horta, L. A., Morrison, E. W., Frey, S. D., Sistla, S. A., & DeAngelis, K. M. (2020). Carbon use efficiency and its temperature sensitivity covary in soil bacteria. *mBio*, 11(1), e02293-19. <https://doi.org/10.1128/mBio.02293-19>

- Pold, G., Grandy, A. S., Melillo, J. M., & DeAngelis, K. M. (2017). Changes in substrate availability drive carbon cycle response to chronic warming. *Soil Biology and Biochemistry*, 110, 68–78.
- Price, P. B., & Sowers, T. (2004). Temperature dependence of metabolic rates for microbial growth, maintenance, and survival. *Proceedings of the National Academy of Sciences*, 101(13), 4631–4636.
- Rasche, F., Knapp, D., Kaiser, C., Koranda, M., Kitzler, B., Zechmeister-Boltenstern, S., Richter, A., & Sessitsch, A. (2011). Seasonality and resource availability control bacterial and archaeal communities in soils of a temperate beech forest. *The ISME Journal*, 5(3), 389–402. <https://doi.org/10.1038/ismej.2010.138>
- Ratkowsky, D. A., Olley, J., McMeekin, T. A., & Ball, A. (1982). Relationship between temperature and growth rate of bacterial cultures. *Journal of Bacteriology*, 149(1), 1–5. doi:10.1128/jb.149.1.1-5.1982
- Robinson, J. M., O'Neill, T. A., Ryburn, J., Liang, L. L., Arcus, V. L., & Schipper, L. A. (2017). Rapid laboratory measurement of the temperature dependence of soil respiration and application to changes in three diverse soils through the year. *Biogeochemistry*, 133(1), 101–112. <https://doi.org/10.1007/s10533-017-0314-0>
- Rocca, J. D., Simonin, M., Blaszczyk, J. R., Ernakovich, J. G., Gibbons, S. M., Midani, F. S., & Washburne, A. D. (2019). The microbiome stress project: Toward a global meta-analysis of environmental stressors and their effects on microbial communities. *Frontiers in Microbiology*, 10(9), 3272.
- Romero-Olivares, A. L., Allison, S. D., & Treseder, K. K. (2017). Soil microbes and their response to experimental warming over time: A meta-analysis of field studies. *Soil Biology and Biochemistry*, 107, 32–40. <https://doi.org/10.1016/j.soilbio.2016.12.026>
- Roy Chowdhury, P., Golas, S. M., Alteio, L. V., Stevens, J. T. E., Billings, A. F., Blanchard, J. L., Melillo, J. M., & DeAngelis, K. (2021). The transcriptional response of soil bacteria to long-term warming and short-term seasonal fluctuations in a terrestrial forest. *Frontiers in Microbiology*, 12, 666558. <https://doi.org/10.3389/fmicb.2021.666558>
- Sanderman, J., & Grandy, A. S. (2020). Ramped thermal analysis for isolating biologically meaningful soil organic matter fractions with distinct residence times. *The Soil*, 6(1), 131–144.
- Sarkar, D. (2008). *Lattice: Multivariate data visualization with R*. Springer.
- Sebag, D., Verrecchia, E. P., Cécillon, L., Adatte, T., Albrecht, R., Aubert, M., Bureau, F., Cailleau, G., Copard, Y., Decaens, T., Disnar, J., Hetényi, M., Nyilas, T., & Trombino, T. (2016). Dynamics of soil organic matter based on new Rock-Eval indices. *Geoderma*, 284, 185–203. <https://doi.org/10.1016/j.geoderma.2016.08.025>
- Simpson, G. L. (2022). permute: Functions for generating restricted permutations of data [Computer software manual]. (R package version 0.9-7).
- Söllinger, A., Séneca, J., Dahl, M. B., Motleleng, L. L., Prommer, J., Verbruggen, E., Sigurdsson, B. D., Janssens, I., Peñuelas, J., Urich, T., Richter, A., & Tveit, A. T. (2022). Down-regulation of the bacterial protein biosynthesis machinery in response to weeks, years, and decades of soil warming. *Science Advances*, 8(12), eabm3230. <https://doi.org/10.1126/sciadv.abm3230>
- Soucémariadin, L., Cécillon, L., Chenu, C., Baudin, F., Nicolas, M., Girardin, C., & Barré, P. (2018). Is Rock-Eval 6 thermal analysis a good indicator of soil organic carbon lability? A method-comparison study in forest soils. *Soil Biology and Biochemistry*, 117, 108–116. doi:10.1016/j.soilbio.2017.10.025
- Spohn, M., Klaus, K., Wanek, W., & Richter, A. (2016). Microbial carbon use efficiency and biomass turnover times depending on soil depth—implications for carbon cycling. *Soil Biology and Biochemistry*, 96, 74–81.
- Sprouffske, K., & Wagner, A. (2016). Growthcurver: An R package for obtaining interpretable metrics from microbial growth curves. *BMC Bioinformatics*, 17(1). <https://doi.org/10.1186/s12859-016-1016-7>
- Torchiano, M. (2020). effsize: Efficient effect size computation [Computer software manual]. (R package version 0.8.1). <https://doi.org/10.5281/zenodo.1480624>
- Van Gestel, N., Shi, Z., Van Groenigen, K. J., Osenberg, C. W., Andresen, L. C., Dukes, J. S., Hovenden, M. J., Luo, Y., Michelsen, A., Pendall, E., Reich, P. B., Schuur, E. A. G., & Hungate, B. A. (2018). Predicting soil carbon loss with warming. *Nature*, 554(7693), E4–E5. <https://doi.org/10.1038/nature25745>
- VandenEnden, L., Anthony, M. A., Frey, S. D., & Simpson, M. J. (2021). Biogeochemical evolution of soil organic matter composition after a decade of warming and nitrogen addition. *Biogeochemistry*, 156(2), 161–175.
- Venables, W. N., & Ripley, B. D. (2002). *Modern applied statistics with S* (4th ed.). Springer.
- Walker, T. W., Janssens, I. A., Weedon, J. T., Sigurdsson, B. D., Richter, A., Peñuelas, J., Leblans, N. I. W., Bahn, M., Bartrons, M., de Jonge, C., Fuchslueger, L., Gargallo-Garriga, A., Gunnarsdóttir, G. E., Marañón-Jiménez, S., Oddsdóttir, E. S., Ostonen, I., Poeplau, C., Prommer, J., Radujković, D., ... Verbruggen, E. (2020). A systemic overreaction to years versus decades of warming in a subarctic grassland ecosystem. *Nature Ecology and Evolution*, 4(1), 101–108. <https://doi.org/10.1038/s41559-019-1055-3>
- Walker, T. W., Kaiser, C., Strasser, F., Herbold, C. W., Leblans, N. I., Woebken, D., Janssens, I. A., Sigurdsson, B. D., & Richter, A. (2018). Microbial temperature sensitivity and biomass change explain soil carbon loss with warming. *Nature Climate Change*, 8(10), 885–889. <https://doi.org/10.1038/s41558-018-0259-x>
- Wardle, D. A., Bardgett, R. D., Klironomos, J. N., Setälä, H., van der Putten, W. H., & Wall, D. H. (2004). Ecological linkages between aboveground and belowground biota. *Science*, 304(5677), 1629–1633. <https://doi.org/10.1126/science.1094875>
- Wickham, H. (2007). Reshaping data with the reshape package. *Journal of Statistical Software*, 21(12), 1–20.
- Wickham, H. (2016). *ggplot2: Elegant graphics for data analysis*. Springer-Verlag.
- Wickham, H., François, R., Henry, L., & Müller, K. (2022). *dplyr: A grammar of data manipulation [computer software manual]*. (R package version 1.0.8).
- Yao, Y., Sun, T., Wang, T., Ruebel, O., Northen, T., & Bowen, B. P. (2015). Analysis of metabolomics datasets with high-performance computing and metabolite atlases. *Metabolites*, 5(3), 431–442.
- Yarwood, S. A., Myrold, D. D., & Hogberg, M. N. (2009). Termination of belowground C allocation by trees alters soil fungal and bacterial communities in a boreal forest. *FEMS Microbiology Ecology*, 70(1), 151–162. <https://doi.org/10.1111/j.1574-6941.2009.00733.x>
- Zhalnina, K., Louie, K. B., Hao, Z., Mansoori, N., da Rocha, U. N., Shi, S., Cho, H., Karaoz, U., Loqué, D., Bowen, B. P., Firestone, M. K., Northen, T. R., & Brodie, E. L. (2018). Dynamic root exudate chemistry and microbial substrate preferences drive patterns in rhizosphere microbial community assembly. *Nature Microbiology*, 3(4), 470–480. <https://doi.org/10.1038/s41564-018-0129-3>

**SUPPORTING INFORMATION**

Additional supporting information can be found online in the Supporting Information section at the end of this article.

**How to cite this article:** Domeignoz-Horta, L. A., Pold, G., Erb, H., Sebag, D., Verrecchia, E., Northen, T., Louie, K., Eloe-Fadrosch, E., Pennacchio, C., Knorr, M. A., Frey, S. D., Melillo, J. M., & DeAngelis, K. M. (2022). Substrate availability and not thermal acclimation controls microbial temperature sensitivity response to long-term warming. *Global Change Biology*, 00, 1–17. <https://doi.org/10.1111/gcb.16544>